

An Infrared High Proper Motion Survey Using 2MASS and SDSS: Discovery of M, L and T Dwarfs

Scott S. Sheppard

*Department of Terrestrial Magnetism, Carnegie Institution of Washington,
5241 Broad Branch Rd. NW, Washington, DC 20015
sheppard@dtm.ciw.edu*

and

Michael C. Cushing

*Institute for Astronomy, University of Hawaii,
2680 Woodlawn Drive, Honolulu, HI 96822*

ABSTRACT

A search of the Two Micron All Sky Survey and Sloan Digital Sky Survey reveals 36 previously unknown high proper motion objects with $J < 17$. Their red-optical colors indicate that 27 are M dwarfs, 8 are early-type L dwarfs, and 1 is a late-type T dwarf. The L dwarfs have $J - K_s$ colors near the extrema of known L dwarfs indicating that previous surveys for L dwarfs using color as a selection criterion may be biased. Followup near-infrared spectroscopy of 6 dwarfs confirm they are all late-type with spectral types ranging from M8 to T4. Spectroscopy also shows that some of the L dwarf spectra exhibit peculiar features similar to other peculiar "blue" L dwarfs which may indicate that these dwarfs have a relatively condensate free atmosphere or may be metal poor. Photometric distance estimates indicate that 22 of the new M, L and T dwarfs lie within 100 pc of the Sun with the newly discovered T dwarf, 2MASS J10595185+3042059, located at ~ 25 pc. Based on the colors and proper motions of the newly identified objects, several appear to be good subdwarf candidates. The proper motions of known ultracool dwarfs detected in our survey were also measured, including, for the first time, SDSS J085834.42+325627.6 (T1), SDSS J125011.65+392553.9 (T4) and 2MASS J15261405+2043414 (L7).

Subject headings: solar neighborhood – stars: distances – stars: late-type – stars: low-mass, brown dwarfs – surveys

1. Introduction

Stars that exhibit high proper motions (HPMs: $\mu > 0''.4 \text{ yr}^{-1}$) are likely to be within the solar neighborhood (less than $\sim 100 \text{ pc}$). Indeed most of our nearest stellar neighbors have been identified through their proper motions using shallow optical surveys such as the Digital Sky Survey (DSS) (Luyten 1979; Wroblewski and Costa 2001; Ruiz et al. 2001; Oppenheimer et al. 2001; Lepine et al. 2003; Teegarden et al. 2003; Hambly et al. 2004; Scholz et al. 2004; Pokorny et al. 2004; Subasavage et al. 2005, Deacon et al. 2005; Lodieu et al. 2005; Finch et al. 2007; Lepine 2008). However, these surveys are not sensitive to the very red ($I - J > 4$), low mass ultracool ($T_{\text{eff}} < 2400 \text{ K}$) L and T dwarfs.

The L and T dwarfs are extremely faint in the optical and to date have only efficiently been identified based on their colors at red optical ($0.6\text{--}1.0 \mu\text{m}$) wavelengths in the Sloan Digital Sky Survey (SDSS: e.g., Fan et al. 2000, Leggett et al. 2002, Chiu et al. 2006) and the Canada France Brown Dwarf Survey (CFBDS: e.g., Delorme et al. 2008) and at near-infrared ($1\text{--}2.5 \mu\text{m}$) wavelengths in the Two Micron All Sky Survey (2MASS: e.g., Kirkpatrick et al. 1999, 2000; Burgasser et al. 2002, 2003b; 2004a; Cruz et al. 2003; Tinney et al. 2005; Kendall et al. 2007;Looper et al. 2007), the Deep Near Infrared Southern Sky Survey (DENIS: Phan-Bao et al. 2008; Kendall et al. 2004) and the UKIRT Infrared Deep Sky Survey (UKIDSS: e.g., Lawrence et al. 2007; Chiu et al. 2008, Pinfield et al. 2008). Because these surveys select ultracool dwarf candidates based on color alone, they may be biased against objects with unusual colors. Metchev et al. (2008) have been able to partially relax this color constraint for low mass objects by comparing the colors of objects in the 2MASS catalog to colors of objects in the SDSS catalog. Although such surveys have proven very successful in identifying L and T dwarfs, it is likely, based on the luminosity function of stellar and substellar objects, that the census of the solar neighborhood within 25 pc remains roughly 20 to 60% deficient (Henry et al. 1997; Henry et al. 2002; Reid et al. 2004; Cruz et al. 2007; Reid et al. 2007).

A search for high proper motions stars at red optical and near infrared wavelengths could 1) potentially identify brown dwarfs in the solar neighborhood via their large proper motions, and 2) remove any potential color bias inherent in most of the surveys conducted to date. Two surveys covering up to a few hundred square degrees have been successful in identifying ultracool dwarfs via proper motion in the near infrared (Artigau et al. 2006; Looper et al. 2008). In this paper, we present a large area survey (~ 8000 square degrees) to search for faint, high proper motion stars in the near infrared using the 2MASS and SDSS catalogs.

2. Target Selection

The 2MASS point source catalog (PSC; Skrutskie et al. 2006) between 0 and 66 degrees declination was compared to the SDSS catalog (York et al. 2000; Pier et al. 2003) within this same range to search for HPM objects. Before comparing the 2MASS and SDSS databases, we performed several cuts on the 2MASS PSC in order to limit the number of candidate HPM objects: 1) The object must be detected in all three filters (J , H and K_s). 2) The J -band magnitude must be brighter than 17th magnitude. 3) The distance between the source and its nearest neighbor in the PSC must be greater than $5''.9$ (a few pixels) to prevent confusion (prox $> 5''.9$). 4) The contamination and confusion flags must be “0” in all three bands to prevent known artifacts or bright nearby objects from giving false positives (cc_flg = 000). 5) The extended source contamination flag must be “0” to indicate the object does not fall within the elliptical boundary of a known extended source (gal_contam = 0). 6) The minor planet flag must be “0” to identify known minor planets (mp_flg = 0). 7) The object can not be identified with a known object within $5''$ from either the USNO-A2.0 or Tycho 2 catalogs (a = 0).

The filtered 2MASS PSC was then compared to the SDSS catalog in order to identify 2MASS point sources that did not have a SDSS source within $2''.35$. This HPM survey covered area from the SDSS using data releases one to five; DR1 (~ 2099 square degrees; Abazajian et al. 2003), DR2 (~ 1225 square degrees; Abazajian et al. 2004), DR3 (~ 1958 square degrees; Abazajian et al. 2005), DR4 (~ 1388 square degrees; Adelman-McCarthy et al. 2006), and DR5 (~ 1330 square degrees; Adelman-McCarthy et al. 2007). In all about 8000 square degrees of sky were covered by the SDSS between DR1 and DR5.

The comparison between the 2MASS and SDSS surveys revealed 1826 objects were cataloged by 2MASS but not cataloged by the SDSS. 1307 of these objects were visually identified as stars in the SDSS images with no detected proper motions between the SDSS and 2MASS data. These stars were not included in the SDSS catalog and thus resulted in false positives. The other 519 objects are candidate HPM objects that were in the 2MASS PSC but had no point sources observed within $2''.35$ in the SDSS data. 357 of the 519 were identified through SIMBAD as known HPM stars and white dwarfs with motions between $0''.2$ and $3''.9 \text{ yr}^{-1}$, 98 were identified as known asteroids that the 2MASS minor planet flag did not register using Lowell Observatory’s asteroid plot program (ASTPLOT; Granvik et al. 2003), 15 were identified through SIMBAD and the Dwarf Archives¹ as known L and T dwarfs (see Table 1). 13 objects (Table 2) could not be correlated with any known SDSS objects or asteroids and thus they are either: 1) Noise or artifacts in the 2MASS catalog,

¹A current list of all known L and T dwarfs is compiled at DwarfArcives.org

2) unknown asteroids, 3) extremely red objects that would not have been detected in the z' , i' or shorter wavelength regime of the SDSS, or 4) extremely fast moving high proper motion objects of well over $10'' \text{ yr}^{-1}$, which is unlikely considering only one known star, Barnard’s Star, has a proper motion this large. All 13 of the unknown objects are very faint with J -band magnitudes well over the 2MASS completeness limit of $J \sim 16$ mag. The main belt asteroid population at these faint magnitudes is probably close to complete though Near Earth Objects (NEOs) are not. As seen in Figure 1, there is no obvious clustering of unidentified objects near the ecliptic as would be expected if most were unknown asteroids. The likely source for each of these unidentified objects is given in Table 2. In addition to comparing the 2MASS and SDSS catalogs we used the Lowell asteroid ephemeris service to determine that the hundreds of 2MASS sources that Burgasser et al. (2003a, 2003b, 2004a) did not detect in their follow-up imaging observations of candidate T dwarfs were indeed asteroids with a few objects being obvious 2MASS artifacts.

The remaining 36 objects in our sample were found to have proper motions between about $0''.2$ and $1''.0 \text{ yr}^{-1}$ but were not in SIMBAD (within $60''$ of the predicted position) or the Dwarf Archives as of 2008 May 1. These 36 objects are thus identified as new HPM objects. Their Proper Motions (PM), Position Angles (PA), and 2MASS J, H, K_s and SDSS r', i' and z' photometry are given in Table 3. We discuss these 36 HPM objects in more detail in the following sections.

3. Analysis

3.1. Survey Results

The proper motions of the 36 newly discovered HPM objects are all less than $1'' \text{ yr}^{-1}$ although objects moving ten times faster would likely have been detected or at least identified as having no SDSS counterpart. The fastest moving non Solar System object detected in this survey was a white dwarf (GJ 518) with a motion of $3''.9 \text{ yr}^{-1}$. Several more known objects, including L and T dwarfs (Table 1), moving well over $1'' \text{ yr}^{-1}$ were also detected.

All the newly discovered HPM objects are quite faint, with many being fainter than 20th magnitude in r' and thus not efficiently detected in earlier optical surveys like the DSS. The colors of the new HPM objects are given in Table 4. $J - K_s$ versus $i' - J$, $r' - i'$ versus $i' - J$, and $J - K_s$ versus $r' - i'$ color-color diagrams are shown in Figures 2 to 4. The large scatter in the $J - K_s$ colors of the L dwarfs (Figure 2) has been ascribed to variations in the properties of their condensate clouds (Tsuji et al. 1996; Knapp et al. 2004), surface gravities (Burrows et al. 2006) and possible unresolved binaries (Liu and Leggett 2005).

This scatter has been found to be even higher for the lower temperature T dwarfs (Dahn et al. 2002; Harris et al. 2003). Figure 3 shows a significant turn over in the object’s $r' - i'$ colors resulting from the formation of Ti-bearing condensates that begin in the late-type M dwarfs (Kirkpatrick et al. 2000; Dahn et al. 2002; Liebert and Gizis 2006).

The rough spectral types for the new HPM objects were estimated using their $i' - J$ colors (Table 4) and a linear fit to known ultracool dwarfs with known spectral types as shown in the Dwarf Archives (Figure 5). We found that the spectral type of an ultracool dwarf is shown to follow the relation

$$\text{SpecType} = -9.4 + 4.7(i' - J) \quad (1)$$

where SpecType is the spectral type of the object with 10=L0, 15=L5, 20=T0, 25=T5 etc. The average spectral typing error using Equation 1 (i.e. the $i' - J$ information) on the sample of objects shown in Figure 5 is about ± 1 sub class. Equation 1 is nearly linear down to at least the early M types ($i' - J \sim 2$; Hawley et al. 2002). Thus even though Equation 1 was determined based on L and early-type T dwarf data covering from $i - J \approx 3.9 - 7.0$, we can extrapolate to bluer colors in order to spectral type M dwarfs.

Since the extremely red ($i' - J \sim 7.8$) object 2MASS J1059+3042² was not detected in the SDSS i' band we estimated its spectral type using its $z' - J$ color. To do so we determined a relation for spectral type versus $z' - J$ colors (Figure 6)

$$\text{SpecType} = -23.0 + 14.2(z' - J) \quad (2)$$

where SpecType is the same as above. This technique is inferior to the $i' - J$ colors technique used above since the z' -band is closer in wavelength to the J-band but is useful for extremely red objects that are difficult to observe in the i' -band. The average spectral typing error using Equation 2 on the sample of objects shown in Figure 6 is about ± 3 sub classes. The spectral types found using Equation 1 or Equation 2 for each of the 36 new HPM objects are given in Table 4.

The approximate absolute magnitude, M_J , of the new HPM objects were estimated by using their $i' - J$ colors and data from Hawley et al. (2002) (see Figure 7)

$$M_J = -9.66 + 15.54(i' - J) - 4.81(i' - J)^2 + 0.72(i' - J)^3 - 0.04(i' - J)^4 \quad (3)$$

and are given in Table 4. Our absolute magnitude calculations are similar to ones used by Cruz et al. (2003) and Phan-Bao et al. (2007) but our analysis allows us to directly relate

²Hereafter we abbreviate the 2MASS and SDSS designations as hhmm±ddmm where the suffix is the sexagesimal right ascension (hours and minutes) and declination (degrees and arcminutes) at J2000.0 equinox.

the $i' - J$ colors to M_J for these newly observed ultracool dwarfs rather than using their unknown spectral types. The absolute magnitudes were used to determine the approximate distances to the objects through, $d = 10^{(J-M_J+5)/5}$ pc. These are very rough estimates for the new HPM objects identified in this survey and assume the objects are single. The distance estimates have uncertainties at about the 25 percent level based on comparing the results with known objects in Table 1. All the objects later than M8 appear to be less than about 100 parsecs from the Earth (Table 4). Several of the early M dwarfs that appear to be at very large distances would have unrealistic tangential velocities ($\gtrsim 500 \text{ km s}^{-1}$). These objects are good subdwarf candidates (see section 4) and thus their absolute magnitudes and distances are likely unreliable since the distance estimates assume the objects to be dwarfs and not subdwarfs. The closest object found in this survey is the T dwarf 2MASS J1059+3042 which lies at a distance of ~ 25 pc if it is a single brown dwarf.

3.2. Survey Consistency

The 2MASS data were taken between 1997 and 2001 (Skrutskie et al. 2006) while the SDSS data acquisition started in 2000 with DR1 and went through DR5, which ended in 2005. Thus the time baseline between DR1 and 2MASS is only a few years (1 to 3 years) while the time baseline for DR5 and 2MASS is several years (up to 8 years). Since most of the new HPM objects are only moving a few tenths of arcseconds per year, they can only be detected in our analysis with a long time baseline and as a result, almost all the new HPM objects discovered in this work were found in the DR5 data release (Figure 1).

As a consistency check we identified 32 L and T dwarfs in the Dwarf Archives with HPM ($> 0''.4 \text{ yr}^{-1}$) that our survey should have detected. We found 15 of these objects (Table 1). We determined that 7 of the 17 objects were not seen in our survey because they had no obvious motion between the 2MASS and SDSS images (the images were taken too close in time) and thus would not be expected to be detected in our survey. One of the 17 objects was located close (about 5 arcminutes) to a nearby bright star ($J \sim 1 \text{ mag}$) and thus was not expected to be detected by our survey because of the large amount of scattered light. Four of the 17 were not clearly detected in the K_s band in the 2MASS data and thus were rejected by our search algorithm. Five of the 17 objects were closer than $2''.35$ to another source in the SDSS data and thus also would have been rejected by our search algorithm. In total we found 100% (15/15) of the known L and T dwarfs that our survey was expected to find. As another measure of the efficiency of our survey, we found about 60% (15/25) of the known L and T dwarfs within our survey that had obvious motion between the 2MASS and SDSS data ($> 2''$).

3.3. Followup Observations

3.3.1. *du Pont*

We observed all 36 objects listed in Table 4 with a Tektronix 2048x2048 CCD ($0''.259$ per pixel) on the du Pont 2.5 meter telescope at Las Campanas, Chile in 2007 Dec, 2008 Feb, and 2008 Mar. These 200 sec *I*-band images confirmed 35 of these objects as having high proper motions. The only object not seen in the *I*-band du Pont data was 2MASS J1059+3042. We thus observed this object in 2008 May with LDSS-3 on the 6.5 meter Magellan telescope in both the *i'*- and *z'*-bands. 2MASS J1059+3042 was easily detected and confirmed as a high proper motion source in two 100 sec *z'*-band exposures. 2MASS J1059+3042 was only marginally detected in one 200 sec *i'*-band exposure demonstrating the extreme redness ($i' - J \sim 7.8$) of this object (Table 4). In addition, we observed all the unidentified objects listed in Table 2 with the du Pont telescope to search for faint *I*-band counterparts that the SDSS would not have detected. These 200 to 600 sec exposures found no obvious objects of interest near any of the locations listed in Table 2.

3.3.2. *IRTF/Spex*

Near-infrared spectra of six of the new HPM objects with estimated spectral types later than M9 V were obtained with SpeX (Rayner et al. 2003) mounted on the 3m NASA Infrared Telescope Facility on 2008 June 13 and 18 (UT). A log of the observations, including the UT date, total integration time, and A0 V standard star are given in Table 5. We used the $0''.5$ -wide slit with the low-resolution prism mode which provides a resolving power of $R \equiv \lambda/\Delta\lambda \approx 150$. A series of 120 sec exposures were obtained at two different positions along the $15''$ -long slit to facilitate sky subtraction. An A0 V standard star with a similar airmass ($\Delta \sec z < 0.1$) was observed after each science target for telluric correction and flux calibration purposes. All observations were conducted at the parallactic angle in order to minimize slit losses and spectral slope variations due to differential atmospheric refraction. Finally, exposures of internal flat field and Ar arc lamps were obtained for flat-fielding and wavelength-calibration purposes.

The data were reduced using Spextool, the data reduction package for SpeX (Cushing et al. 2004). The package performs nonlinearity corrections, flat-fielding, optimal extraction of spectra, and wavelength calibration. The spectra were then corrected for telluric absorption and flux calibrated using the observed A0 V standard star and the technique described in Vacca et al. (2003). The spectra of the 6 candidates are shown in Figure 8. The S/N of the spectra range from 20 to 200 except for 2MASS J1230+2827 which ranges from 10 to 50.

Five of the six dwarfs exhibit features typical of late-type M and L dwarfs including broad H₂O absorption at ~ 1.4 and $\sim 1.8 \mu\text{m}$, the Wing-Ford FeH band head at $0.99 \mu\text{m}$, K I and Na I doublets from 1.15 to $1.3 \mu\text{m}$, and the CO overtone band heads at $\sim 2.29 \mu\text{m}$. The extremely red object ($i' - J \sim 7.8$), 2MASS J1059+3042, exhibits CH₄ absorption bands at 1.2 , 1.6 , and $2.2 \mu\text{m}$ indicating that it is a T dwarf.

Spectral types for the 6 dwarfs were determined in two ways. First, each spectrum was compared to the ~ 250 spectra of M, L, and T dwarfs (obtained with the same instrument setup as our data) in the SpeX Prism Spectral Library³. The best fitting library spectrum for each dwarf was found by minimizing the sum of the squared residuals between our spectrum and the library spectra (after all spectra are normalized to unity over the 2.1 to $2.2 \mu\text{m}$ wavelength range) and are overplotted in Figure 8. 2MASS J1059+3042 is well matched by the T4 near-infrared standard 2MASS J2254188+312349 (Burgasser et al. 2006) so we assign it a spectral type of T4. The remaining 5 dwarfs are well matched by their respective library spectra, but assigning them spectral types by direct comparison is difficult since there are no spectral standards for M and L dwarfs in the near-infrared; the spectral types given in Figure 8 were derived from red optical data. We have therefore also derived the spectral types of the 5 M and L dwarfs using various spectral indices from the literature (Reid et al. 2001, Testi et al. 2001, Burgasser et al. 2002, 2006, 2007b, 2008, Allers et al. 2007) as well as the Geballe et al. (2002) indices that are used to define near-infrared L dwarf subtypes. The resulting spectral types are given in Table 6 and a summary of the spectral types derived by the various methods are given in Table 7. With the exception of 2MASS J1059+3042, the spectral types derived by the various methods are in reasonable agreement.

4. Discussion

The original goal of this survey was to identify brown dwarfs that were close to the Sun and to understand whether or not there is a color bias in previous surveys that use color as a selection criterion. Although no brown dwarfs located very close to the Sun were identified, our results suggest that a color bias does exist in current surveys. As shown in Figure 2, six of the eight L dwarfs identified in this survey have $J - K_s$ colors that lie at the extrema of the distribution of L dwarfs colors. Followup spectroscopy shows that 2MASS J1431+1436 and 2MASS J1434+2202 appear to have anomalous spectral features given their (tentative) spectral types. Based on their $J - K_s$ colors alone, both dwarfs would have a spectral type of earlier than M9 V (Kirkpatrick 2008) indicating that these

³<http://www.browndwarfs.org/spexprism>

dwarfs are much bluer than typical L dwarfs. Indeed Burgasser et al. (2004a, 2008a) have noted that the spectra of 2MASS J0041–3547 and SIPS J0921–2104, the best fitting library spectra for 2MASS J1431+1436 and 2MASS J1434+2202 respectively, appear anomalous with stronger FeH absorption, weaker CO absorption, and a bluer near-infrared continuum than typical L dwarfs. Such spectral characteristics have been previously ascribed to subsolar metallicities (e.g., Cruz et al. 2007), high surface gravities or variations in the condensate clouds properties (e.g., Burgasser et al. 2008a). A sub solar metallicity may explain the peculiar nature of 2MASS J1434+2202 given that the spectral type of its best fitting library spectrum, 2MASS J0041–3547, is sdM9.

Most of the newly discovered objects are relatively distant (Table 4). It is thus likely that most of these objects have large tangential velocities in order for them to show such high proper motions at relatively large distances. Metal poor subdwarfs are usually associated with large tangential velocities. In order to determine if any of the objects reported in this survey are subdwarfs we calculated their Reduced Proper Motions, RPM. The RPM of each object was determined using the relation $RPM = r' + 5 + 5 \log \mu$ (Salim and Gould 2002; Subasavage et al. 2005; Marshall 2008). The RPM can be thought of as a rough luminosity class (or absolute magnitude) using only proper motion (μ) and apparent magnitude (r') by assuming they are directly related. This assumption is usually valid though many factors make the scatter in the relationship large. The RPM is a simple technique to allow identification of object types that differ from the normal main sequence. This technique is useful when looking for a crude way to identify white dwarfs and subdwarfs since they will have bluer colors or fainter RPMs for a given color.

In Figure 9 we plot the $r' - J$ colors versus the RPM for the newly discovered high proper motion objects discovered in this survey along with some white dwarfs found in this survey, the L4 subdwarf 2MASS J1626+3925 also found in this survey and several confirmed M subdwarfs seen in both the SDSS and 2MASS from Marshall (2008) and Lepine and Scholz (2008). It can clearly be seen that the white dwarfs occupy the far left in the figure while the subdwarfs occupy the center and lower portions of Figure 9. Several of our newly identified HPM objects are near the center and lower portions of Figure 9 and are thus good subdwarf candidates (see Table 4). In fact, 2MASS J1434+2202, which is near the known subdwarf 2MASS J1626+3925 in Figure 9, has been identified as a likely subdwarf from our near-infrared spectroscopy (see Table 7). Most of our newly found HPM objects are on the far right of Figure 9 and thus not likely subdwarfs and are definitely not white dwarfs. Because the scatter is rather large a more detailed spectroscopic observational campaign will be required to determine which of these objects are subdwarfs.

5. Summary

About 8000 square degrees from the 2MASS and SDSS catalogs were compared to find low mass (red), high proper motion objects. Thirty-six new HPM objects were discovered in the analysis. All objects were confirmed as having high proper motions with deep imaging at the du Pont 2.5 meter and Magellan 6.5 meter telescopes. Their red optical and near infrared colors indicate that 27 are M dwarfs, 8 are early-type L dwarfs, and 1 is a late-type T dwarf. Through comparing the colors and reduced proper motions of our newly identified HPM objects we find several are good subdwarf candidates.

The newly identified L dwarfs appear to have $J - K_s$ colors at the extreme of known L dwarf colors. This may hint at a slight color bias in brown dwarf detections through color surveys. Followup near-infrared spectroscopy of six of the late-type objects show that 2MASS J14313097+1436539 and 2MASS J14343616+2202463 exhibit peculiar spectral features similar to other peculiar “blue” L dwarfs. Spectroscopy also shows that 2MASS 14343616+2202463 could be an L subdwarf and 2MASS 10595185+3042059 is a T dwarf. From their estimated absolute magnitudes it appears all of the brown dwarfs found in this survey are within 100 parsecs of the Earth.

In addition, several hundred previously known high proper motion objects were also detected as well as ten known L- and five known T-dwarfs. For the first time we determined the proper motions and position angles for known T-dwarfs SDSS J085834.42+325627.6 and SDSS J125011.65+392553.9 as well as the late L-dwarf 2MASS J15261405+2043414.

An additional 13 objects that appeared real in the 2MASS catalog but are not identified or correlated with any objects in the SDSS were found. Deep du Pont 2.5 meter I -band imaging of these locations found no interesting counterparts. These objects are likely artifacts in the 2MASS catalog but could be extremely red objects that could not be detected in the shorter wavelength SDSS images or very fast moving objects of well over $10''$ per year.

Acknowledgments

We thank Alan Tokunaga for granting us director’s discretionary time on the IRTF. This research has benefitted from the M, L, and T dwarf compendium housed at DwarfArchives.org and maintained by Chris Gelino, Davy Kirkpatrick, and Adam Burgasser and the SpeX Prism Spectral Libraries, maintained by Adam Burgasser at <http://www.browndwarfs.org/spexpr>. This paper includes data gathered with the 6.5 meter Magellan Telescopes located at Las Campanas Observatory, Chile. This publication makes use of data products from the Two Micron All Sky Survey, which is a joint project of the University of Massachusetts and

the Infrared Processing and Analysis Center/California Institute of Technology, funded by the National Aeronautics and Space Administration and the National Science Foundation. The SDSS is managed by the Astrophysical Research Consortium for the Participating Institutions. The Participating Institutions are the American Museum of Natural History, Astrophysical Institute Potsdam, University of Basel, Cambridge University, Case Western Reserve University, University of Chicago, Drexel University, Fermilab, the Institute for Advanced Study, the Japan Participation Group, Johns Hopkins University, the Joint Institute for Nuclear Astrophysics, the Kavli Institute for Particle Astrophysics and Cosmology, the Korean Scientist Group, the Chinese Academy of Sciences (LAMOST), Los Alamos National Laboratory, the Max-Planck-Institute for Astronomy (MPIA), the Max-Planck-Institute for Astrophysics (MPA), New Mexico State University, Ohio State University, University of Pittsburgh, University of Portsmouth, Princeton University, the United States Naval Observatory, and the University of Washington. Funding for the SDSS and SDSS-II has been provided by the Alfred P. Sloan Foundation, the Participating Institutions, the National Science Foundation, the U.S. Department of Energy, the National Aeronautics and Space Administration, the Japanese Monbukagakusho, the Max Planck Society, and the Higher Education Funding Council for England. The SDSS web site is <http://www.sdss.org>.

REFERENCES

- Abazajian, D., Adelman, J., Agueros, M. et al. 2003, *AJ*, 126, 2081
- Abazajian, D., Adelman, J., Agueros, M. et al. 2004, *AJ*, 128, 502
- Abazajian, D., Adelman, J., Agueros, M. et al. 2005, *AJ*, 129, 1755
- Adelman-McCarthy, J., Agueros, M., Allam, S. et al. 2006, *ApJS*, 162, 38
- Adelman-McCarthy, J., Agueros, M., Allam, S. et al. 2007, *ApJS*, 172, 634
- Allers, K. N., et al. 2007, *ApJ*, 657, 511
- Artigau, E., Doyon, R., Lafreniere, D., Nadeau, D., Robert, J. and Albert, L. 2006, *ApJ*, 651, L57
- Burgasser, A., Kirkpatrick, J., Brown, M., et al. 2002, *ApJ*, 564, 421
- Burgasser, A., Kirkpatrick, J., McElwain, M., Cutri, R., Burgasser, A. and Skrutskie, M. 2003a, *AJ*, 125, 850
- Burgasser, A., McElwain, M., Kirkpatrick, J. 2003b, *AJ*, 126, 2487
- Burgasser, A., McElwain, M., Kirkpatrick, J., Cruz, K., Tinney, C. and Reid, N. 2004a, *AJ*, 127, 2856

- Burgasser, A. et al. 2004b, *ApJ*, 604, 827
- Burgasser, A., Geballe, T., Leggett, S., Kirkpatrick, J., Golimowski, D. 2006, *ApJ*, 637, 1067
- Burgasser, A., Cruz, K. and Kirkpatrick, J. 2007a, *ApJ*, 657, 494
- Burgasser, A. J., Looper, D. L., Kirkpatrick, J. D., & Liu, M. C. 2007b, *ApJ*, 658, 557
- Burgasser, A., Looper, D., Kirkpatrick, J., Cruz, K. and Swift, B. 2008a, *ApJ*, 674, 451
- Burgasser 2008b, submitted
- Burgasser, A. J., Looper, D. L., Kirkpatrick, J. D., Cruz, K. L., & Swift, B. J. 2008, *ApJ*, 674, 451
- Burrows, A. et al. 2006, *ApJ*, 640, 1063
- Chiu, K., Fan, X., Leggett, S., Golimowski, D., Zheng, W., Geballe, T., Schneider, D. and Brinkmann, J. 2006, *AJ*, 131, 2722
- Chiu, K., Liu, M., Jiang, L. et al. 2008, *MNRAS*, 385, L53
- Cruz, K., Reid, N., Liebert, J., Kirkpatrick, J. and Lowrance, P. 2003, *AJ*, 126, 2421
- Cruz, K., Reid, N., Kirkpatrick, J., et al. 2007, *AJ*, 133, 439
- Cushing, M. C., Vacca, W. D., and Rayner, J. T. 2004, *PASP*, 116, 362
- Cushing, M., Rayner, J., and Vacca, W. 2005, *ApJ*, 623, 1115
- Dahn, C. et al. 2002, *AJ*, 124, 1170
- Deacon, N., Hambly, N. and Cooke, J. 2005, *AA*, 435, 363
- Delorme, P. et al. 2008, *AA*, 484, 469
- Fan, X., et al. 2000, *AJ*, 119, 928
- Finch, C., Henry, T., Subasavage, J., Jao, W. and Hambly, N. 2007, *AJ*, 134, 252
- Geballe, T., Knapp, G., Leggett, S. et al. 2002, *ApJ*, 564, 466
- Gizis, J., Monet, D., Reid, N. et al. 2000, *AJ*, 120, 1085
- Granvik, M., Virtanen, J., Muinonen, K., Bowell, E., Koehn, B. and Tancredi, G. 2003, *Earth, Moon and Planets*, 92, 73
- Hambly, N., Henry, T., Subasavage, J., Brown, M., and Jao, W. 2004, *AJ*, 128, 437
- Harris, H., Conard, D., Frederick, V. et al. 2003, *IAU Symposium* 211, 409
- Hawley, S., Covey, K., Knapp, G. et al. 2002, *AJ*, 123, 3409
- Henry, T., Ianna, P., Kirkpatrick, J. and Jahreiss, H. 1997, *ApJ*, 114, 388
- Henry, T., Walkowicz, L., Barto, T. and Golimowski, D. 2002, *AJ*, 123, 2002

- Jameson, R., Casewell, S., Bannister, N. et al. 2008, MNRAS, 384, 1399
- Kendall, T., Delfosse, X., Martin, E. and Forveille, T. 2004, AA, 416, L17
- Kendall, T., Jones, H., Pinfield, D. et al. 2007, MNRAS, 374, 445
- Kirkpatrick, J. D., Henry, T. J., & McCarthy, D. W., Jr. 1991, ApJS, 77, 417
- Kirkpatrick, J., Reid, N., Liebert, J. et al. 1999, ApJ, 519, 802
- Kirkpatrick, J. et al. 2000, AJ, 120, 447
- Kirkpatrick, J. D. 2008, 14th Cambridge Workshop on Cool Stars, Stellar Systems, and the Sun, 384, 85
- Knapp, G. et al. 2004, AJ, 127, 3553
- Lawrence, A., Warren, S., Almaini, O. et al. 2007, MNRAS, 379, 1599
- Leggett, S. K., et al. 2002, ApJ, 564, 452
- Lepine, S., Shara, M. and Rich, R. 2003, AJ, 126, 921
- Lepine, S. 2008, AJ, 135, 2177
- Lepine, S. and Scholz, R. 2008, ApJ, 681, L33
- Liebert, J. and Gizis, J. 2006, PASP, 118, 659
- Liu, M. and Leggett, S. 2005, ApJ, 634, 616
- Lodieu, N., Scholz, R., McCaughrean, M., Ibata, R., Irwin, M. and Zinnecker, H. 2005, AA, 440, 1061
- Looper, D., Kirkpatrick, J. and Burgasser, A. 2007, AJ, 134, 1162
- Looper, D., et al. 2008, ApJ, in press (astro-ph 0806.1059)
- Luyten, W. 1979, LHS Catalogue (2nd ed.; Minneapolis: Univ. Minnesota Press)
- Marshall, J. 2008, AJ, 135, 1000
- Metchev, S. Kirkpatrick, J., Berriman, B., Looper, D. 2008, ApJ, 676, 1281
- Oppenheimer, B., Hambly, N., Digby, A., Hodgkin, S. and Saumon, D. 2001, Science, 292, 698
- Phan-Bao, N., Bessell, M., Martin, E. et al. 2008, MNRAS, 383, 831
- Pier, J., Munn, J., Hindsley, R., Hennessy, G., Kent, S., Lupton, R. and Ivezić, Z. 2003, AJ, 125, 1559
- Pinfield, D. J., et al. 2008, ArXiv e-prints, 806, arXiv:0806.0294
- Pokorny, R., Jones, H., Hambly, N. and Pinfield, D. 2004, AA, 421, 763

- Rayner, J. T., Toomey, D. W., Onaka, P. M., Denault, A. J., Stahlberger, W. E., Vacca, W. D., Cushing, M. C., and Wang, S. 2003, *PASP*, 115, 362
- Reid, I. N., Burgasser, A. J., Cruz, K. L., Kirkpatrick, J. D., & Gizis, J. E. 2001, *AJ*, 121, 1710
- Reid, N., Cruz, K., Allen, P. et al. 2004, *AJ*, 128, 463
- Reid, N., Cruz, K. and Allen, P. 2007, *AJ*, 133, 2825
- Ruiz, M., Wischnjewsky, M., Rojo, P. and Gonzalez, L. 2001, *ApJS*, 133, 119
- Salim, S. and Gould, A. 2002, *ApJ*, 575, 83
- Schmidt, S., Cruz, K., Bongiorno, B., Liebert, J. and Reid, N. 2007, 133, 2258
- Scholz, R., Lehmann, I., Matute, I. and Zinnecker, H. 2004, *AA*, 425, 519
- Skrutskie, M., Cutri, R., Stiening, R. et al. 2006, *AJ*, 131, 1163
- Subasavage, J., Henry, T., Hambly, N., Brown, M. and Wei-Chun, J. 2005, *AJ*, 129, 413
- Teegarden, B. et al. 2003, *ApJ*, 589, L51
- Testi, L., et al. 2001, *ApJ*, 552, L147
- Tinney, C., Burgasser, A., Kirkpatrick, J. and McElwain, M. 2005, *AJ*, 130, 2326
- Tsuji, T., Ohnaka, K. and Aoki, W. 1996, *AA*, 305, L1
- Vacca, W. D., Cushing, M. C., and Rayner, J. T. 2003, *PASP*, 115, 389
- Vrba, F., Henden, A., Luginbuhl, C. et al. 2004, *AJ*, 127, 2948
- Wilson, J., Miller, N., Gizis, J. et al. 2003, *IAU Symposium* 211, 197
- Wroblewski, H. and Costa, E. 2001, *AA*, 367, 725
- York, D., Adelman, J., Anderson, J. et al. 2000, *AJ*, 120, 1579

Table 1. Properties of Known L and T Dwarfs Detected in this Survey

Name	PM ^a (" / yr)	PA ^b (deg)	J^c (mag)	$i' - J$ (mag)	Spec. ^d Type	Ref. ^e
2MASS J14213145+1827407	0.79	257	13.23	4.2	L0	9,10,17
2MASS J14392836+1929149	1.34	288	12.76	4.4	L1	2,12
2MASS J13004255+1912354	1.48	213	12.72	4.5	L1	9,10,11
2MASS J15065441+1321060	1.14	269	13.37	4.6	L3	9,13
2MASS J16154416+3559005	0.53	184	14.54	4.6	L3	1,13
2MASS J16262034+3925190	1.79	279	14.44	3.5	sdL4	8,16
2MASS J13285503+2114486	0.50	150	16.20	5.2	L5	2,12
2MASS J15150083+4847416	2.04	328	14.11	5.2	L6	13,14,15
2MASS J15261405+2043414	0.43*	216*	15.59	5.0	L7	1
2MASS J08251968+2115521	0.62	241	15.10	5.5	L7.5	1,2,3
SDSS J085834.42+325627.6	0.76*	272*	16.45	5.6	T1	4
SDSS J125011.65+392553.9	1.03*	182*	16.54	> 5.5	T4	4
2MASS J12314753+0847331	1.51	228	15.57	> 6.4	T5.5	6,8
2MASS J09373487+2931409	1.68	143	14.65	> 7.3	T6p	5,6,7
2MASS J15530228+1532369	0.44	294	15.83	> 6.2	T7	5,6,13

*Indicates this is the first time that this type of measurement for this object has been published.

^aThe Proper Motion (PM) of the object as observed between the 2MASS and SDSS data. Uncertainties are at about the 10 percent level.

^bThe Position Angle (PA) of the motion. Uncertainties are generally about 1 degree.

^cThe J -band photometry from 2MASS. Uncertainties are less than 0.1 magnitudes.

^dThe spectral types of the L dwarfs are based on red optical spectroscopy and are on the Kirkpatrick et al. (1999) system. The spectral types of the T dwarfs are based on near-infrared spectroscopy and are on the Burgasser et al. (2006) system. The spectral type for 2MASS J16262034+3925190 is tentative (Burgasser et al. 2007a).

^eReferences for discovery, spectral type identification, proper motion and position angle measurements if applicable:

References. — 1) Kirkpatrick et al. (2000), 2) Dahn et al. (2002), 3) Knapp et al. (2004), 4) Chiu et al. (2006), 5) Burgasser et al. (2002), 6) Burgasser et al. (2006), 7) Vrba et al. (2004), 8) Burgasser et al. (2004a), 9) Gizis et al. (2000), 10) Schmidt et al. (2007), 11) Burgasser et al. (2008), 12) Kirkpatrick et al. (1999), 13) Jameson et al. (2008), 14) Wilson et al. (2003), 15) Cruz et al. (2007), 16) Burgasser, Cruz, and Kirkpatrick (2007), 17) Reid et al. in preparation.

Table 2. Objects in the 2MASS PSC but not in the SDSS PSC^a

2MASS Name	J^b (mag)	H^b (mag)	K_s^b (mag)	JD ^d	Comments ^c
J00461651+1419298	16.9	16.3	15.9	2451437.8263	Diff
J08204794+2440364	16.9	16.2	15.8	2451506.9024	Diff
J09581895+0143068	16.8	16.8	16.1	2451577.7483	Noise
J10385877+2718553	16.9	16.3	15.7	2450873.8665	Diff
J11254075+5029579	16.5	16.2	15.8	2451601.7506	Diff
J11280132+0715387	16.9	17.2	15.9	2451605.6786	Noise
J13165176+1338169	16.8	16.4	16.3	2451526.0489	Noise
J13300094+4912080	16.9	16.8	16.4	2451621.8835	Noise
J14510138+2847574	16.5	16.1	15.3	2451335.6506	Diff
J15490517+1542418	16.9	16.6	16.0	2451557.0605	Noise
J16382286+2501307	16.9	16.5	16.2	2451621.9096	Noise
J17262351+2708338	16.6	16.3	15.5	2451628.9394	Diff
J23390347+1415329	16.9	16.4	16.1	2451877.6576	Noise

^aThese are objects that were not linked to known asteroids, not seen in the SDSS and were not obvious artifacts or noise. These objects were cataloged by 2MASS in J , H and K_s . The above objects are all near the detection limit of 2MASS. Most of the objects are likely artifacts from scattered light of nearby bright stars but some could be unknown asteroids, extremely red objects ($i' - J > 7$ mags) or extremely high proper motion stars or brown dwarfs ($>> 10'' \text{ yr}^{-1}$). Deep I -band imaging of these areas with the Dupont 2.5 meter telescope found no objects near any of the coordinates listed above.

^bThe J , H and K_s photometry from 2MASS. Most of these objects are near the limit of 2MASS detection and thus their uncertainties are higher than most 2MASS photometry and are generally between 0.2 and 0.4 magnitudes.

^cMost of these objects are likely artifacts in the 2MASS data and here we comment on what they likely are: Diff = Differential diffraction spike from nearby bright star or Noise = Background Noise.

^dThe Julian Date of the 2MASS image and coordinates.

Table 3. New High Proper Motion Objects^a

2MASS Name	PM ^b (""/yr)	PA ^c (deg)	r' ^d (mag)	i' ^d (mag)	z' ^d (mag)	J ^e (mag)	H ^e (mag)	K_s ^e (mag)	JD ^f
2MASS J08404809+2024121	0.43	121	22.2	19.2	17.6	15.78 ± 0.06	15.16 ± 0.08	14.7 ± 0.1	2451106.0059
2MASS J09122241+2258119	0.36	221	20.1	17.9	16.7	15.22 ± 0.04	14.78 ± 0.05	14.4 ± 0.1	2450825.8190
2MASS J09585080+2001525	0.38	223	22.7	20.5	18.6	16.08 ± 0.08	15.25 ± 0.08	14.6 ± 0.1	2450838.7923
2MASS J10001708+3218306	0.45	240	23.7	21.0	18.7	16.62 ± 0.12	15.70 ± 0.11	15.4 ± 0.2	2450893.7960
2MASS J10120045+2046128	0.44	242	19.7	18.3	17.5	16.21 ± 0.07	15.69 ± 0.09	15.7 ± 0.2	2450839.8136
2MASS J10182596+2710554	0.35	177	21.3	18.2	16.6	14.81 ± 0.03	14.30 ± 0.05	14.0 ± 0.1	2450868.8630
2MASS J10340305+2008184	0.34	189	20.4	17.5	15.9	14.00 ± 0.02	13.40 ± 0.03	13.0 ± 0.0	2450841.8812
2MASS J10351535+2736016	0.41	153	19.8	18.5	17.8	16.45 ± 0.10	15.92 ± 0.13	15.8 ± 0.2	2450873.8263
2MASS J10512777+1816421	0.40	144	20.0	18.7	17.9	16.72 ± 0.14	15.71 ± 0.14	15.8 ± 0.2	2450842.9695
2MASS J10543739+1426556	0.68	252	21.9	19.3	18.0	16.48 ± 0.12	15.85 ± 0.14	15.9 ± 0.2	2451261.7513
2MASS J10595185+3042059	0.53	184	...	24.0	19.8	16.21 ± 0.09	15.80 ± 0.12	15.6 ± 0.2	2450893.8534
2MASS J11092121+4425488	0.73	234	18.0	16.8	16.3	14.97 ± 0.05	14.50 ± 0.04	14.5 ± 0.1	2451266.7371
2MASS J11101471+1731121	0.37	269	21.5	18.6	17.1	15.02 ± 0.03	14.32 ± 0.03	14.0 ± 0.0	2450800.0062
2MASS J11212384+2018192	0.68	246	21.7	18.7	17.1	15.20 ± 0.04	14.64 ± 0.05	14.2 ± 0.1	2450846.8717
2MASS J11261886+4429311	0.57	167	20.6	18.5	17.4	15.93 ± 0.06	15.40 ± 0.08	15.6 ± 0.1	2451247.7611
2MASS J11303803+2341480	0.57	256	23.3	21.3	19.1	16.65 ± 0.13	15.87 ± 0.12	15.7 ± 0.2	2451525.9601
2MASS J11355548+2639401	0.64	229	19.2	17.3	16.3	14.84 ± 0.04	14.31 ± 0.04	14.0 ± 0.1	2451579.8211
2MASS J11470670+1729029	0.38	252	20.8	18.1	16.4	14.22 ± 0.03	13.57 ± 0.03	13.1 ± 0.0	2450822.9444
2MASS J11541839+2248569	0.44	166	20.3	18.6	17.7	16.30 ± 0.09	15.60 ± 0.11	15.1 ± 0.1	2451260.8033
2MASS J12205687+2132371	0.51	170	20.6	17.8	16.3	14.47 ± 0.03	13.97 ± 0.03	13.6 ± 0.0	2450948.6895
2MASS J12304562+2827583	0.58	263	22.4	20.1	18.5	16.07 ± 0.09	15.00 ± 0.08	14.4 ± 0.1	2451653.7353
2MASS J12353360+1805024	0.47	281	19.3	17.1	15.9	14.41 ± 0.03	13.91 ± 0.04	13.7 ± 0.0	2451293.6837
2MASS J12370037+2107445	0.54	273	19.9	17.1	15.6	13.58 ± 0.03	12.96 ± 0.02	12.6 ± 0.0	2451293.6962
2MASS J12373441+3028596	0.74	313	23.8	20.5	18.6	16.37 ± 0.14	16.27 ± 0.31	15.5 ± 0.2	2450876.9792
2MASS J12531161+2728145	0.53	151	21.2	18.4	16.6	14.49 ± 0.04	13.84 ± 0.04	13.3 ± 0.0	2451555.9499
2MASS J12572875+1555356	0.58	160	19.7	17.8	16.8	15.29 ± 0.04	14.87 ± 0.06	14.5 ± 0.1	2450836.9610
2MASS J13001921+2036407	0.50	289	20.0	17.5	16.3	14.47 ± 0.03	13.89 ± 0.03	13.5 ± 0.0	2451261.8390
2MASS J13034203+2158519	0.87	179	19.8	17.3	16.0	14.33 ± 0.03	13.79 ± 0.03	13.6 ± 0.0	2451261.8670
2MASS J13512249+1419168	0.60	246	21.6	19.1	18.0	16.43 ± 0.10	16.07 ± 0.19	15.7 ± 0.2	2450935.7796
2MASS J13580384+1458204	0.51	298	22.3	20.5	18.9	16.37 ± 0.11	15.25 ± 0.11	14.7 ± 0.1	2451531.0524
2MASS J14005107+2142014	0.41	193	19.7	17.8	16.8	15.18 ± 0.05	14.83 ± 0.08	14.5 ± 0.1	2450953.8086
2MASS J14222455+2834542	0.56	261	21.0	18.1	16.7	14.83 ± 0.04	14.36 ± 0.04	14.0 ± 0.1	2451264.9276
2MASS J14313097+1436539	0.43	259	22.3	19.7	17.6	15.15 ± 0.04	14.50 ± 0.05	14.1 ± 0.1	2450935.8401
2MASS J14343616+2202463	0.83	286	21.6	18.8	16.8	14.52 ± 0.04	13.83 ± 0.04	13.6 ± 0.0	2451557.0310
2MASS J15052821+3115037	0.53	184	19.1	17.7	17.0	15.58 ± 0.15	14.99 ± 0.07	14.8 ± 0.1	2450897.9287
2MASS J17143190+3544160	0.13	345	21.9	19.6	18.2	16.42 ± 0.11	16.15 ± 0.21	15.7 ± 0.2	2450913.9061

^aObjects that were found in both 2MASS and SDSS catalogs, moved > 2.35 arcseconds and were not in the SIMBAD database or known brown dwarfs on the dwarf archives page (dwarfarchives.org) as of May 1, 2008. 2MASS astrometry is good to about 80 mas (Skrutskie et al. 2006).

^bThe Proper Motion (PM) of the object as observed between the 2MASS and SDSS data. Uncertainties are at about the 10 percent level.

^cThe Position Angle (PA) of the objects motion. Uncertainties are generally about 1 degree.

^dThe r' , i' and z' photometry from the SDSS. Uncertainties are generally well below 0.1 magnitudes. The only exception is the i' photometry for 2MASS J10595185+3042059. This object was not seen in the i' SDSS data and was only marginally detected in one 200 second image using LDSS3 on the 6.5 meter Clay telescope. Thus the uncertainty in the i' -band photometry for 2MASS J10595185+3042059 is around 0.3 magnitudes.

^eThe J, H and K photometry from 2MASS.

^fThe Julian Date (JD) of the 2MASS image and coordinates.

Table 4. Colors and Distances of Newly Identified High Proper Motion Objects

2MASS Name	$r' - i'$ (mag)	$i' - J$ (mag)	$J - K_s$ (mag)	RPM ^a	M_J ^b (mag)	D ^c (pc)	Spec ^d Type
2MASS J11092121+4425488	1.2 ± 0.1	1.83 ± 0.05	0.50 ± 0.08	21.4*	6.5*	500*	M0
2MASS J10512777+1816421	1.3 ± 0.1	1.93 ± 0.15	0.92 ± 0.27	20.5*	7.0*	860*	M1
2MASS J10351535+2736016	1.4 ± 0.1	2.03 ± 0.11	0.65 ± 0.21	20.4*	7.3*	90*	M1
2MASS J10120045+2046128	1.4 ± 0.1	2.06 ± 0.09	0.52 ± 0.19	20.6*	7.5*	550*	M1
2MASS J15052821+3115037	1.4 ± 0.1	2.10 ± 0.05	0.80 ± 0.11	21.0*	7.7*	400*	M1
2MASS J11541839+2248569	1.7 ± 0.1	2.28 ± 0.10	1.16 ± 0.15	21.2*	8.2*	60*	M2
2MASS J11355548+2639401	1.9 ± 0.1	2.45 ± 0.05	0.83 ± 0.06	22.0	8.7	170	M3
2MASS J12572875+1555356	1.9 ± 0.1	2.46 ± 0.05	0.78 ± 0.08	21.9	8.7	205	M3
2MASS J14005107+2142014	2.0 ± 0.1	2.57 ± 0.07	0.68 ± 0.17	20.2	9.0	170	M3
2MASS J11261886+4429311	2.1 ± 0.1	2.58 ± 0.05	0.30 ± 0.11	22.8	9.1	230	M3
2MASS J12353360+1805024	2.2 ± 0.1	2.64 ± 0.04	0.72 ± 0.05	20.5	9.2	110	M3
2MASS J09122241+2258119	2.2 ± 0.1	2.68 ± 0.06	0.83 ± 0.06	20.0	9.3	155	M4
2MASS J13512249+1419168	2.5 ± 0.1	2.68 ± 0.10	0.75 ± 0.26	24.0	9.2	275	M4
2MASS J10543739+1426556	2.6 ± 0.1	2.80 ± 0.14	0.62 ± 0.28	25.0*	9.5*	250*	M5
2MASS J13034203+2158519	2.6 ± 0.1	2.92 ± 0.04	0.76 ± 0.04	24.1	9.8	80	M5
2MASS J13001921+2036407	2.5 ± 0.1	3.03 ± 0.04	0.95 ± 0.05	21.5	10.0	80	M5
2MASS J17143190+3544160	2.3 ± 0.1	3.20 ± 0.14	0.70 ± 0.25	16.8	10.2	170	M6
2MASS J12205687+2132371	2.8 ± 0.1	3.28 ± 0.04	0.88 ± 0.05	22.2	10.4	65	M6
2MASS J14222455+2834542	2.9 ± 0.1	3.30 ± 0.04	0.82 ± 0.06	23.1	10.4	75	M7
2MASS J10182596+2710554	3.1 ± 0.1	3.37 ± 0.06	0.84 ± 0.06	21.1	10.5	70	M7
2MASS J08404809+2024121	3.1 ± 0.2	3.39 ± 0.09	1.05 ± 0.13	23.0	10.6	110	M8
2MASS J12370037+2107445	2.8 ± 0.1	3.49 ± 0.04	1.02 ± 0.04	21.8	10.7	40	M8
2MASS J11212384+2018192	3.0 ± 0.1	3.50 ± 0.07	1.00 ± 0.07	24.7	10.7	80	M8
2MASS J10340305+2008184	2.9 ± 0.1	3.52 ± 0.05	1.00 ± 0.04	20.1	10.8	45	M8
2MASS J11101471+1731121	2.9 ± 0.1	3.56 ± 0.06	1.07 ± 0.05	21.6	10.8	70	M8
2MASS J11470670+1729029	2.7 ± 0.1	3.89 ± 0.05	1.12 ± 0.04	21.0	11.3	40	M9
2MASS J12531161+2728145	2.8 ± 0.1	3.91 ± 0.06	1.14 ± 0.05	23.1	11.4	40	M9
2MASS J12304562+2827583	2.3 ± 0.2	4.02 ± 0.10	1.63 ± 0.11	24.7	11.5	80	L0
2MASS J12373441+3028596	3.3 ± 0.3	4.10 ± 0.11	0.90 ± 0.25	27.3	11.6	90	L0
2MASS J13580384+1458204	1.8 ± 0.2	4.10 ± 0.11	1.71 ± 0.14	23.9	11.6	90	L0
2MASS J14343616+2202463	2.8 ± 0.1	4.28 ± 0.04	0.97 ± 0.06	25.6*	11.9*	35*	L1
2MASS J09585080+2001525	2.3 ± 0.2	4.38 ± 0.11	1.46 ± 0.11	22.9	12.1	65	L2
2MASS J10001708+3218306	2.7 ± 0.6	4.40 ± 0.15	1.20 ± 0.14	24.7	12.1	80	L2
2MASS J14313097+1436539	2.6 ± 0.1	4.54 ± 0.04	1.02 ± 0.07	23.0	12.3	40	L2
2MASS J11303803+2341480	2.0 ± 0.2	4.61 ± 0.15	0.90 ± 0.22	25.5*	12.4*	70*	L3
2MASS J10595185+3042059	...	7.80 ± 0.31	0.67 ± 0.21	31.8	14.1	25	T8

^aThe Reduced Proper Motion (RPM) of the objects. An object with an * indicates it is a good subdwarf candidate (see Figure 9). If it is a subdwarf then the absolute magnitude and distance estimates are unreliable.

^bApproximate absolute magnitude based on the $i' - J$ color information as described in Hawley et al. (2002). Uncertainties are a few tenths of magnitudes based on comparing the results for known objects from Table 1. An object with an * indicates it is a good subdwarf candidate (see Figure 9). If it is a subdwarf then the absolute magnitude and distance estimates are unreliable.

^cEstimated distances for the objects are good to about the 25 percent level based on comparing the results to known objects from Table 1. An object with an * indicates it is a good subdwarf candidate (see

Figure 9). If it is a subdwarf then the absolute magnitude and distance estimates are unreliable.

^dThe spectral type is estimated based on the $i' - J$ colors as shown in Figure 5. The estimated spectral type based on the $i' - J$ colors is likely accurate to within a subclass except for 2MASS 1059+3042 which is good to within about 3 subclasses since the $z' - J$ colors were used to find the spectral type for this extremely red object.

Table 5. Log of SpeX Observations

Object	UT Date	Exp. Time (sec)	A0 V
2MASS J1059+3042	2008 Jun 13	1200	HD 89239
2MASS J1230+2827	2008 Jun 18	1440	HD 107655
2MASS J1237+3028	2008 Jun 18	1200	HD 107655
2MASS J1253+2728	2008 Jun 18	1200	HD 107655
2MASS J1431+1436	2005 Jun 18	1200	HD 121880
2MASS J1434+2202	2008 Jun 18	960	HD 121880

Table 6. Spectral Indices of Late M and Early L Dwarfs

Index	Spectral Type				
	2MASS 1230	2MASS 1237	2MASS 1253	2MASS 1431	2MASS 1434
Reid et al. (2001)					
H ₂ O ^A	M9 V	M7.5 V	L0.5	L5.5	L3.5
H ₂ O ^B	L1.5	M8 V	L0	L4.5	L3.5
Testi et al. (2001)					
sH ₂ O ^J	L3	<L0	L0	L1.5	L0.5
sH ₂ O ^{H1}	L1.5	<L0	L0	L4	L2.5
sH ₂ O ^{H2}	<L0	L0	L2	L5.5	L5
sH ₂ O ^K	L1	<L0	<L0	L2.5	L1.5
Burgasser et al. (2002)					
H ₂ O-A	L1.5	M6.5 V	M8 V	L2	L0.5
H ₂ O-B	M8.5 V	M6.5 V	M8.5 V	L6	L4
H ₂ O-C	L2	M5 V	M8 V	L5.5	L2
Geballe et al. (2002)					
H ₂ O 1.5 μ m	L0	<L0	<L0	<L0	<L0
CH ₄ 2.2 μ m	L3	L4	<L3	<L3	L4
Burgasser et al. (2006,2007)					
H ₂ O-J	L2.5	L0	L0.5	L3.5	L3.5
H ₂ O-H	M9.5	<L0	<L0	L1	L0
CH ₄ -K	L1.5	L2.5	L0.5	<L0	L3
Allers et al. (2007)					
H ₂ O	L0.5	M7.5 V	M8.5 V	L3.5	L2
Burgasser et al. (2008)					
H ₂ O(c)	L3.5	M8 V	L0	L2.5	L0
Mean Sp. Type ^a	L1 \pm 1.5	M8.5 V \pm 2.5	M9.5 V \pm 1	L3.5 \pm 1.5	L2.5 \pm 1.5

^aMean spectral type not including upper limits (e.g., <L0). The error is the RMS error.

Table 7. Summary of Spectral Types for Objects Observed with SpeX

Object	Spectral Types		
	$i' - J$	Direct Comparison	Spectral Indices
2MASS J1059+3042	T8	T4	...
2MASS J1230+2827	L0	L2	$L1 \pm 1.5$
2MASS J1237+3028	L0	M7.5 V	$M8.5 \pm 2.5$
2MASS J1253+2728	M9 V	M8.5 V	$M9.5 V \pm 1$
2MASS J1431+1436	L2	L2	$L3.5 \pm 1.5$
2MASS J1434+2202	L1	sdM9	$L2.5 \pm 1.5$

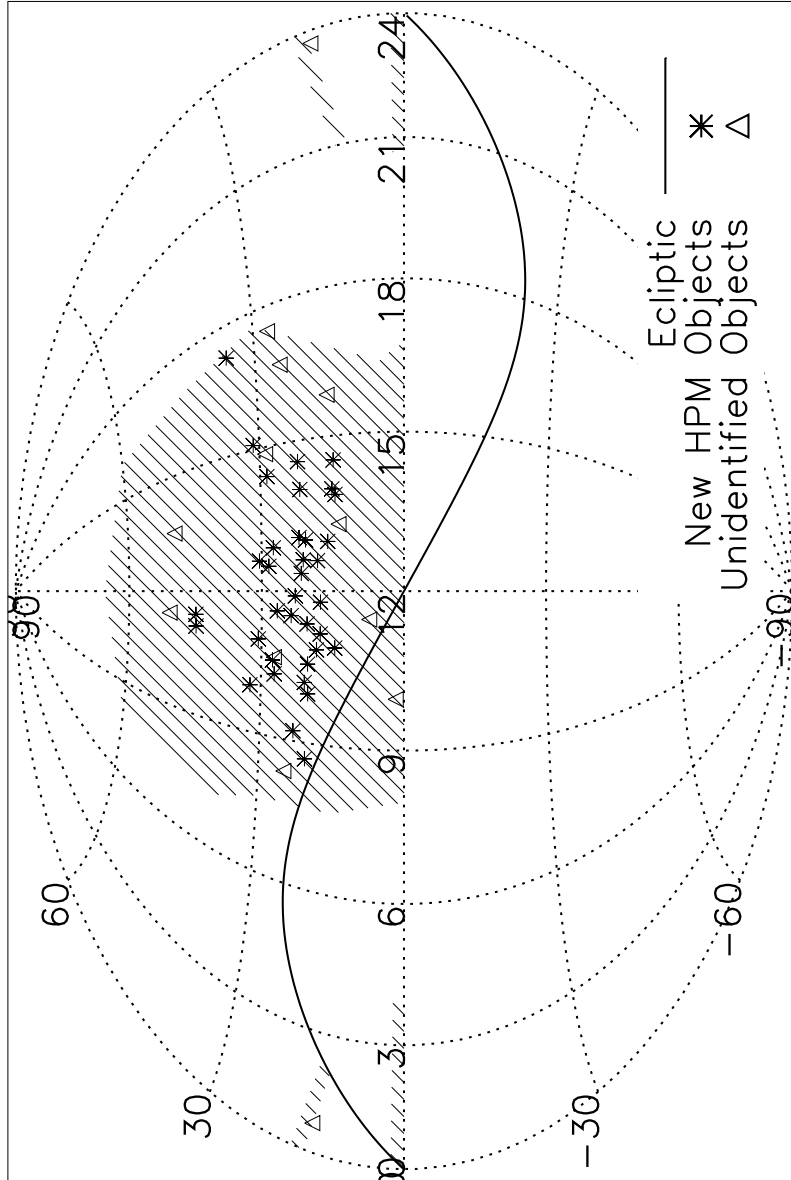


Fig. 1.— The location of newly identified high proper motion objects with declination in degrees on the vertical axis and right ascension in hours on the horizontal axis. The shaded area is the 8000 square degrees where the 2MASS and SDSS data overlapped. Most of the 36 newly identified HPM objects are between about 15 and 30 degrees declination since this is where the SDSS Data Release 5 (DR5) was focused. The DR5 has the longest time baseline between the 2MASS and SDSS images allowing for the more numerous slower proper motion objects to be identified. The 13 2MASS objects that do not have an identified SDSS source (open triangles) are likely artifacts in the 2MASS catalog but could be unknown asteroids, extremely red objects, or extremely high proper motion objects. Since the triangles are uncorrelated with the ecliptic (solid line) its unlikely they are unknown asteroids.

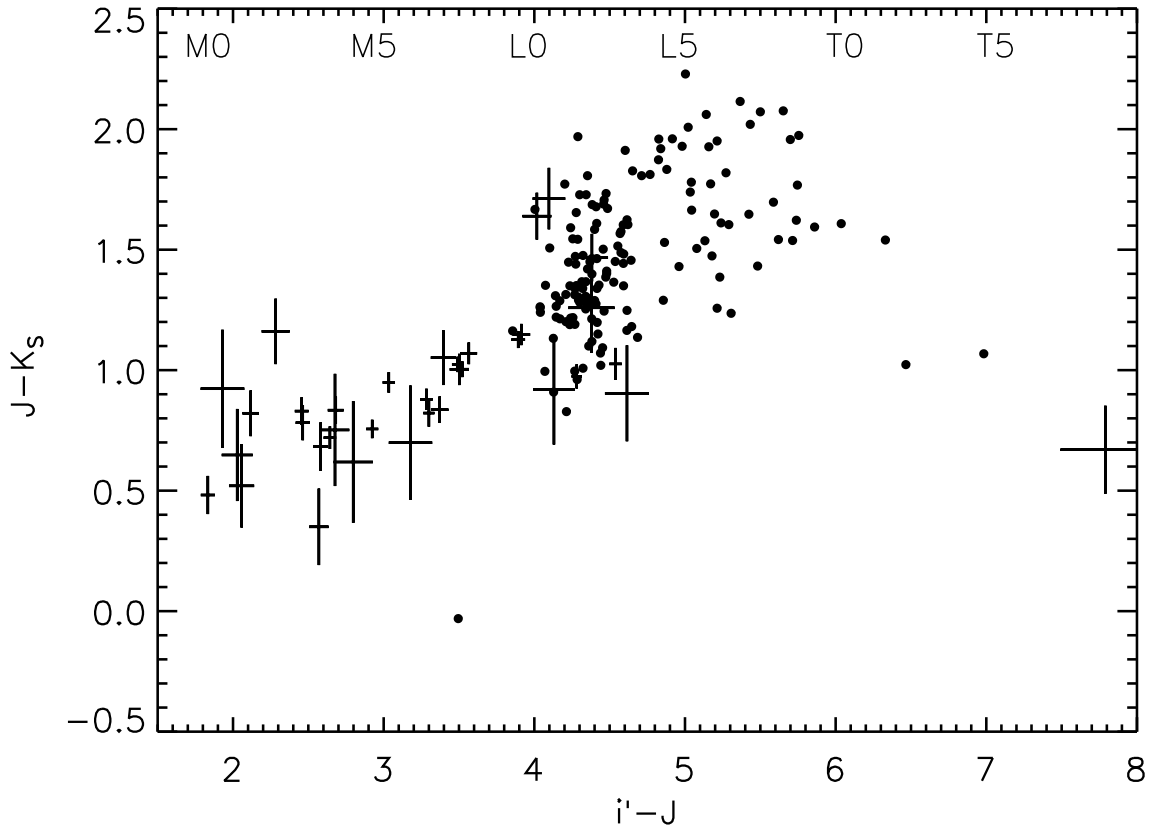


Fig. 2.— The $i' - J$ versus the $J - K_s$ colors of the 36 newly discovered high proper motion objects (plus signs). Also plotted are the known ultracool dwarfs with spectral types L0 or later observed in the SDSS (filled circles) as of 2008 May 1. All colors were obtained through the 2MASS and SDSS point source catalogs. Approximate spectral types based on the average $i' - J$ colors of M, L, and T dwarfs are given (see text). It is apparent that most of the new candidate L dwarfs have $J - K_s$ colors that lie at the extrema of the known early-type L dwarfs suggesting a possible bias in the sample of known L dwarfs that were identified based on their colors alone. The T dwarf candidate is at the right. T dwarfs are extremely faint in the i' band and thus very few have been observed in the SDSS. The known brown dwarf in the lower center of this figure is the L4 subdwarf, 2MASS J16262034+3925190 (Burgasser et al. 2004b).

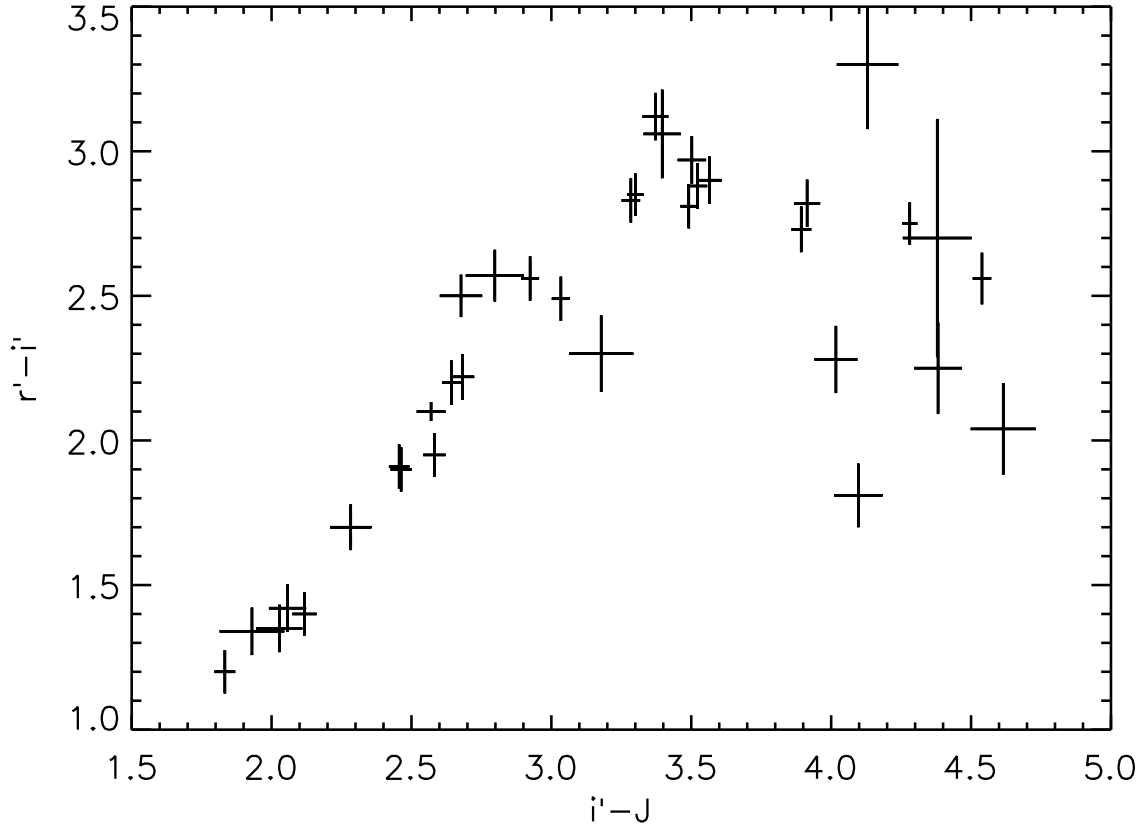


Fig. 3.— The $i' - J$ versus $r' - i'$ colors of the 36 newly discovered high proper motion objects. There is an obvious turn over near $r' - i' \sim 3$ and $i' - J \sim 4$. This turn over has been associated with Ti-bearing condensates that begin in late-type M dwarfs (Kirkpatrick et al. 2000; Dahn et al. 2002; Liebert and Gizis 2006). The T dwarf candidate is not in this figure because its r' magnitude is unknown.

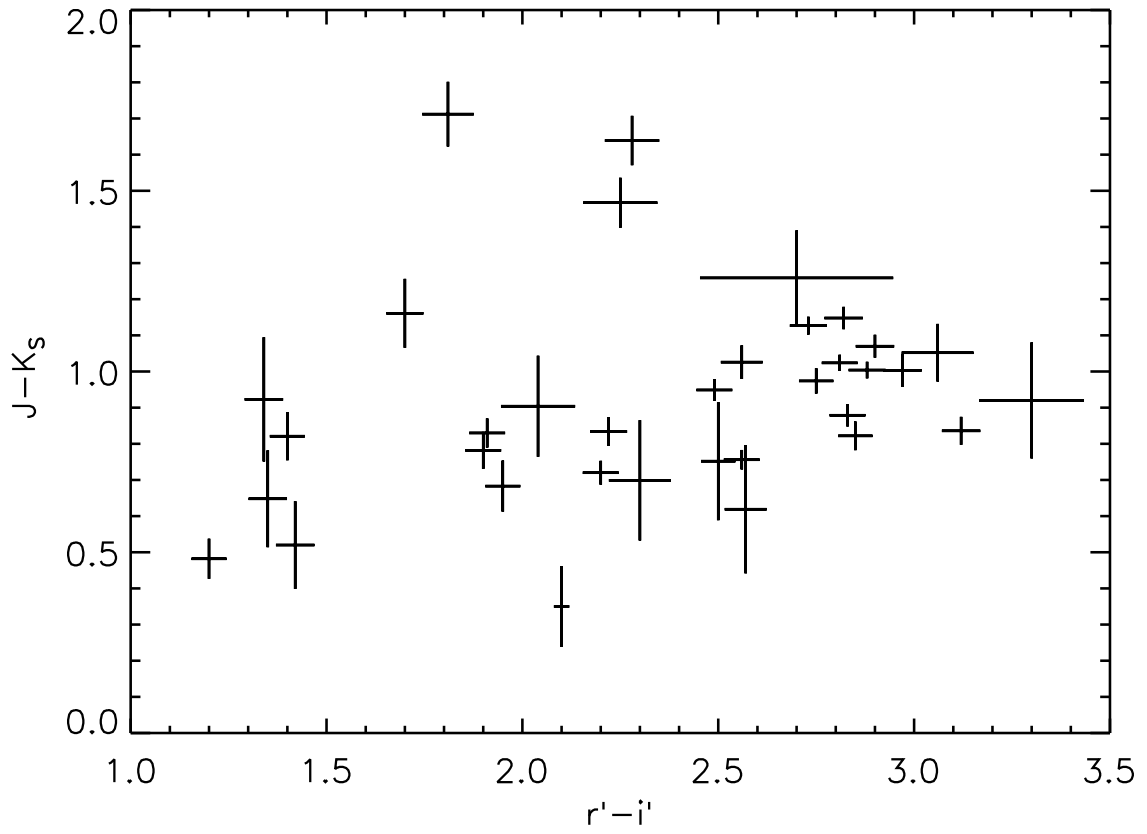


Fig. 4.— The $r' - i'$ versus $J - K_s$ colors of the 36 newly discovered high proper motion objects. The T dwarf candidate is not in this figure because its r' magnitude is unknown.

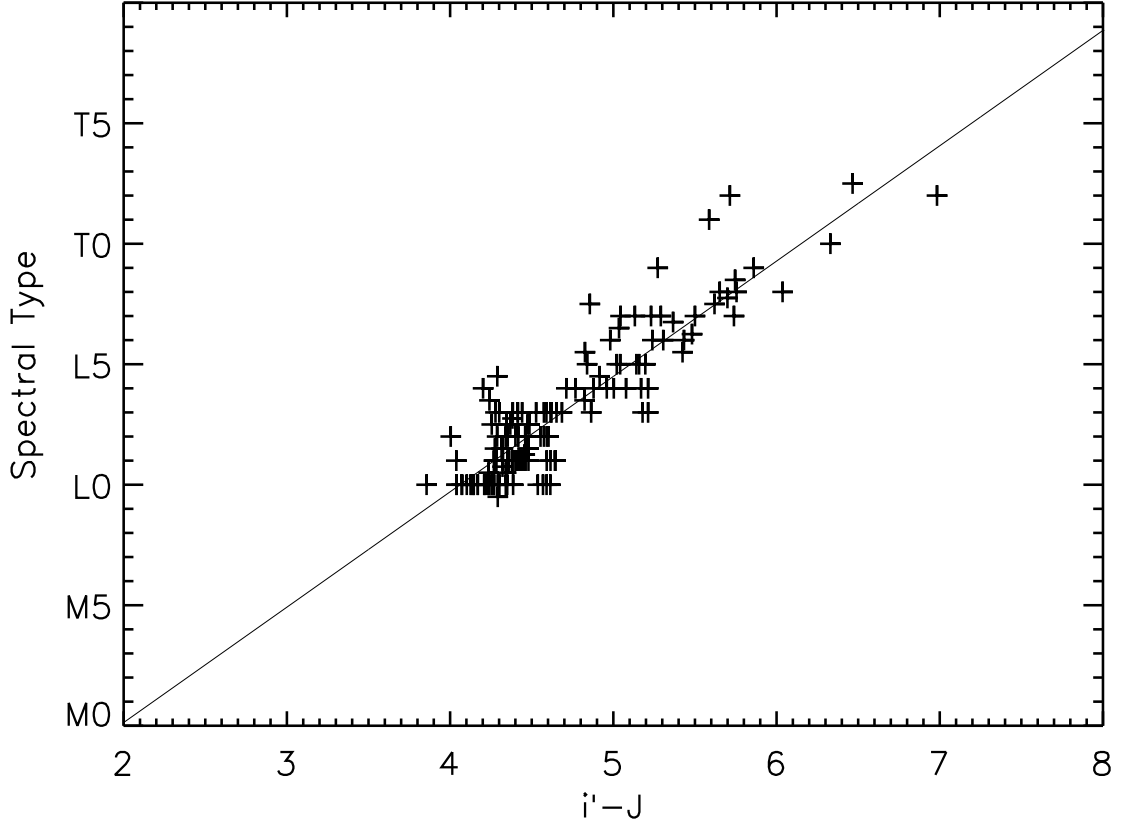


Fig. 5.— The $i' - J$ colors versus spectral type of known L and T dwarfs detected by the SDSS. All ultracool dwarfs plotted had their photometry taken from the SDSS and 2MASS data bases exactly as the 36 newly discovered objects found in this work to allow a direct comparison. The solid line is the best fit to the data and is used to estimate the spectral types of the newly observed objects (Table 4). The linear spectral type fit found for brown dwarfs using $i' - J$ is: $\text{SpecType} = -9.4 + 4.8(i' - J)$, where the Spectral Type is 05=M5, 10=L0, 15=L5, 20=T0, 25=T5 etc. Because T dwarfs are extremely faint in the i' band few have been reliably observed in the SDSS. As shown by Hawley et al. (2002) this linear fit is good down to the earliest M type dwarfs. We extrapolate the spectral type based on the linearity of the fit for objects that have a $i' - J$ color less than 3.9 and greater than 7 magnitudes.

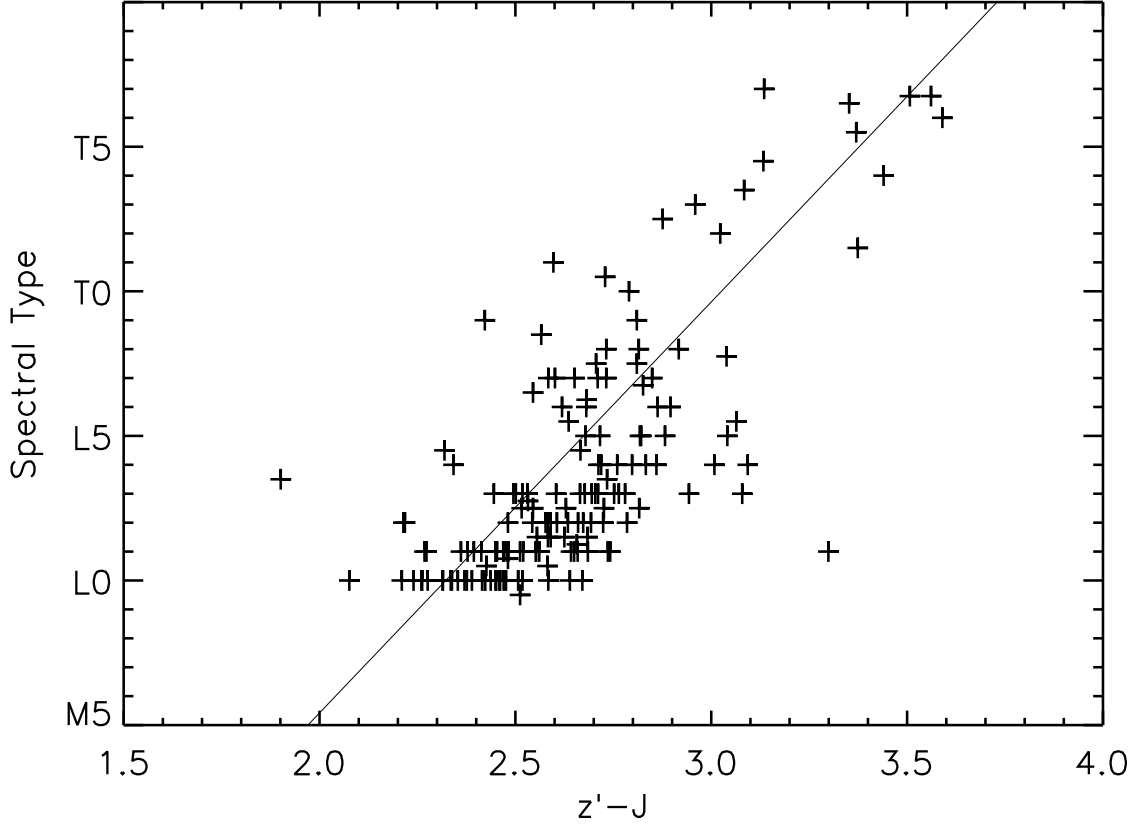


Fig. 6.— The $z' - J$ colors versus spectral type of known L and T dwarfs observed with the SDSS and 2MASS (see dwarfarchives.org). The solid line is the best fit to the data and is used to estimate the spectral type of the newly discovered T dwarf 2MASS J10595185+3042059 (Table 4). Determining the spectral type through the $z' - J$ color technique is good for late-type T dwarfs because i' band detections are rare in the SDSS. The linear spectral type fit found for brown dwarfs using $z' - J$ is: $\text{SpecType} = -23.0 + 14.2(z' - J)$, where the Spectral Type is 05=M5, 10=L0, 15=L5, 20=T0, 25=T5 etc.

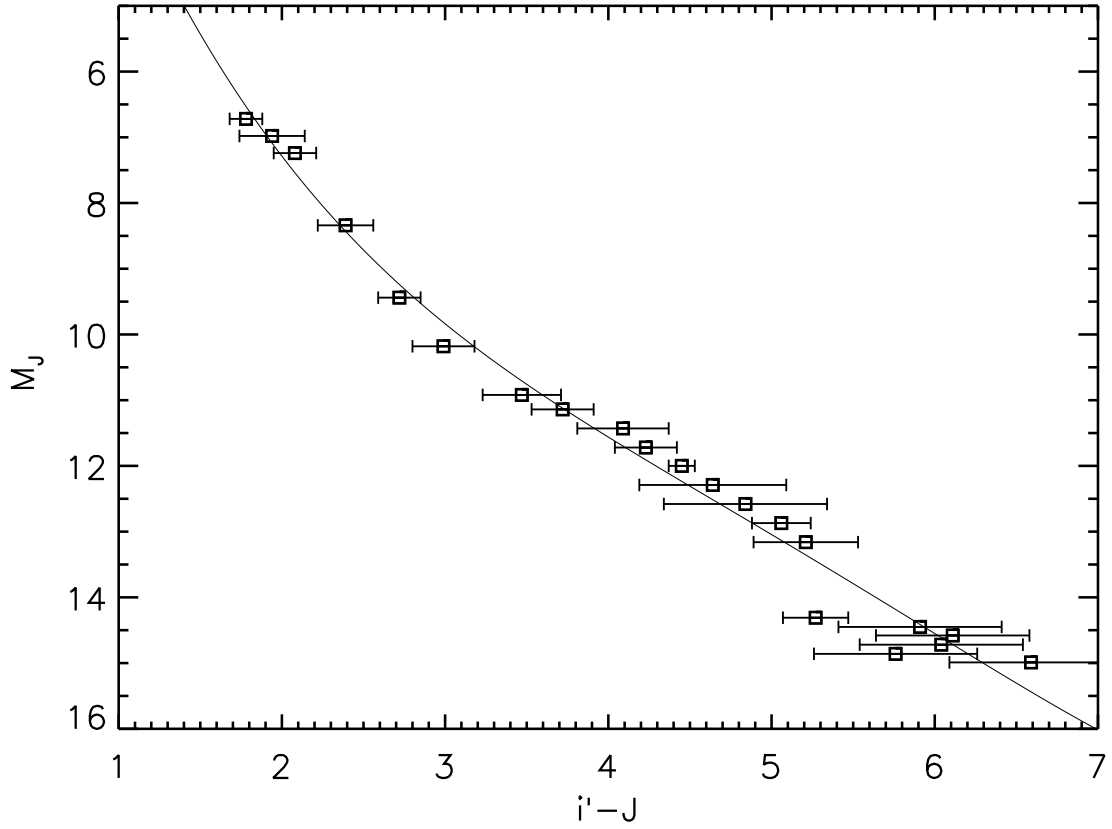


Fig. 7.— The fitted $i' - J$ versus absolute magnitude using data points from Hawley et al. (2002). This fit is used to determine the absolute magnitude, M_J , of the newly identified high proper motion objects using their $i' - J$ magnitudes: $M_J = -9.66 + 15.54(i' - J) - 4.81(i' - J)^2 + 0.72(i' - J)^3 - 0.04(i' - J)^4$

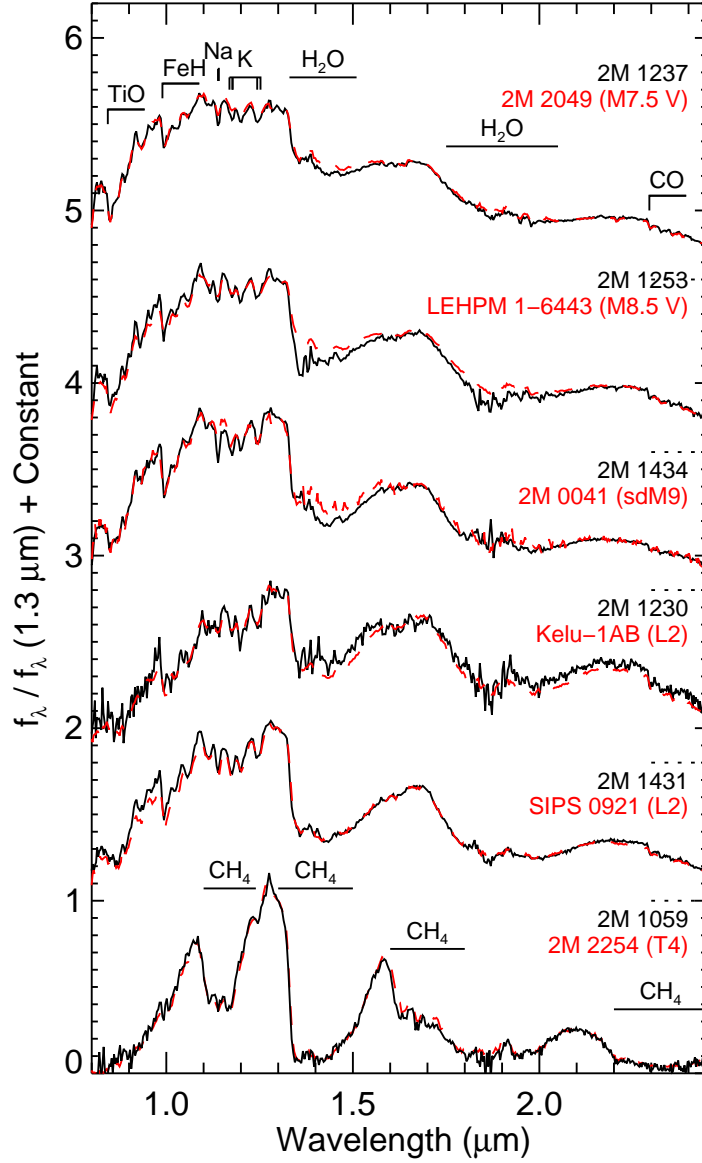


Fig. 8.— The 0.8–2.45 μm spectra (black) of 2MASS J1237+3028, 2MASS J1253+2728, 2MASS J1434+2202, 2MASS J1230+2827, 2MASS J1431+1436, and 2MASS J1059+3042. Overplotted (red) are the best fitting spectra in the SpeX Prism Spectral Library, 2MASS J2049–1944 (Burgasser et al. 2004a), LEHPM 1–6443 (Burgasser (2008b), 2MASS J0041+3547 (Burgasser et al. (2004a), Kelu-1AB (Burgasser et al. 2007b), SIPS 0921+2104 (Burgasser et al. 2007b) and 2MASS 2254+3123 (Burgasser et al. (2004a). The spectra are normalized to unity at 1.3 μm and offset by constants (dotted lines). Prominent atomic and molecular absorption features are indicated.

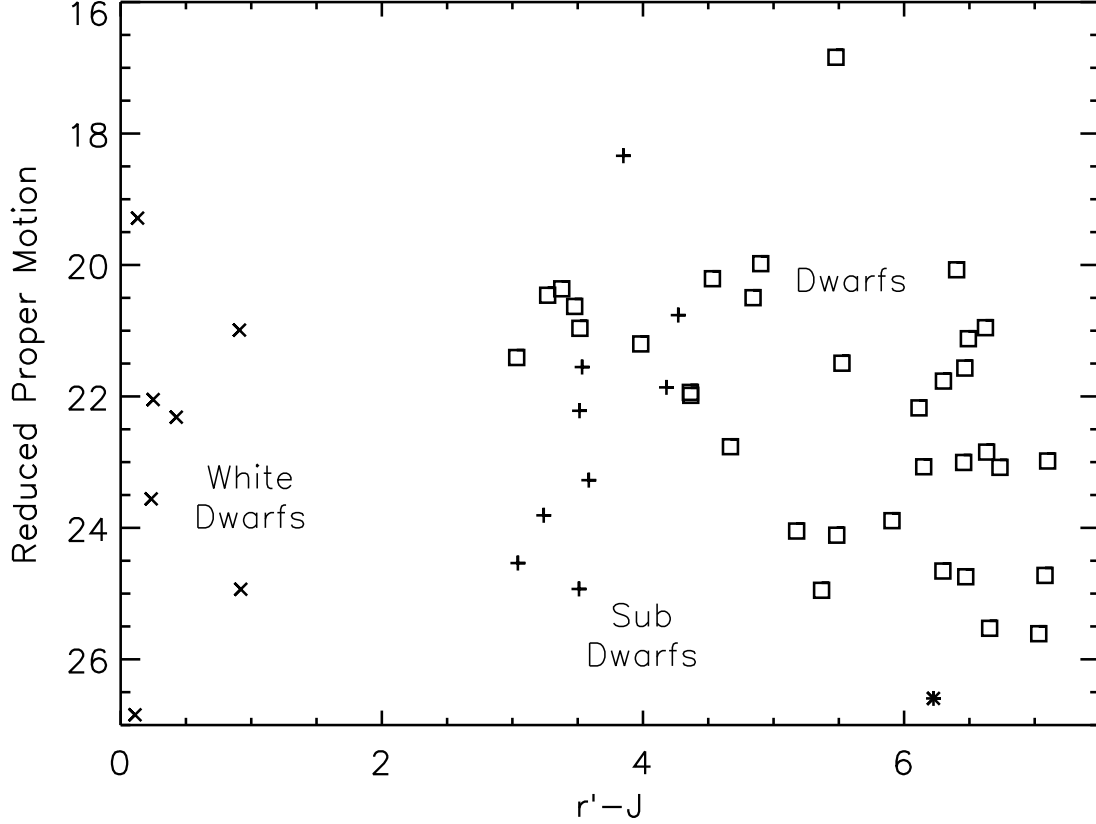


Fig. 9.— The $r' - J$ colors versus the reduced proper motion (RPM) for the 36 newly identified high proper motion objects (squares), white dwarfs discovered in this survey (x's), known M subdwarfs (plus signs) as found in the SDSS and confirmed by Marshall (2008) and Lepine and Scholz (2008) and the known L4 subdwarf 2MASS J1626+3925 (asterisk) that was detected in this survey and identified as a subdwarf by Burgasser et al. (2007). The white dwarfs occupy the left portion of the figure and none of the newly identified HPM objects are near this region. The subdwarfs occupy the center and lower portions of the figure. Several of the newly identified HPM objects are near the subdwarf region and thus are good subdwarf candidates (see Table 4). 2MASS J1434+2202 was identified as a possible L subdwarf from followup spectroscopy and is the bottom most point at the far right of this figure near the known L subdwarf 2MASS J1626+3925. Most of the newly identified HPM objects are in the far right of this figure which indicates that most are dwarf type objects. The one T dwarf discovered in this survey is not shown since its r' magnitude is unknown.